## Title

Overlapping and Distinct Roles of Aspergillus fumigatus UDP-glucose 4-Epimerases in Galactose Metabolism and the Synthesis of Galactose-containing Cell Wall Polysaccharides* * This work was supported, in whole or in part, by National Institutes of He...



## Journal

Journal of Biological Chemistry, 289(3)

## ISSN

0021-9258

## Authors

Lee, Mark J
Gravelat, Fabrice N
Cerone, Robert P
et al.

## Publication Date

2014

## DOI

10.1074/jbc.m113.522516

THE JOURNAL OF BIOLOGICAL CHEMISTRY VOL. 289, NO. 3, pp. 1243–1256, January 17, 2014


# Overlapping and Distinct Roles of *Aspergillus fumigatus* UDP-glucose 4-Epimerases in Galactose Metabolism and the Synthesis of Galactose-containing Cell Wall Polysaccharides*

Received for publication, October 8, 2013, and in revised form, November 15, 2013 Published, JBC Papers in Press, November 20, 2013, DOI 10.1074/jbc.M113.522516

**Mark J. Lee[‡1], Fabrice N. Gravelat[‡], Robert P. Cerone[‡], Stefanie D. Baptista[‡], Paolo V. Campoli[‡], Se-In Choe[‡], Ilia Kravtsov[‡], Evgeny Vinogradov[§], Carole Creuzenet[¶], Hong Liu[‖], Albert M. Berghuis[**], Jean-Paul Latgé[‡‡], Scott G. Filler[‖], Thierry Fontaine[‡‡], and Donald C. Sheppard[‡2]**

*From the [‡]Department of Microbiology and Immunology, McGill University, Montréal, Québec H3A 2B4, Canada, the [§]National Research Council, Ottawa, Ontario K1A 0R6, Canada, the [¶]Department of Microbiology and Immunology, University of Western Ontario, London, Ontario N6A 5C1, Canada, the [‖]Division of Infectious Diseases, Los Angeles Biomedical Medical Institute at Harbor-University of California, Los Angeles Medical Center, Torrence, California 90502, the [**]Department of Biochemistry, McGill University, Montréal, Québec H3A 2B4, Canada, and the [‡‡]Aspergillus Unit, Institut Pasteur, 75724 Paris, France*

**Background:** *Aspergillus fumigatus* produces two galactose-containing exopolysaccharides, galactomannan and galactosaminogalactan.
**Results:** Galactosaminogalactan synthesis requires the UDP-glucose 4-epimerases, Uge5 and Uge3, whereas galactomannan synthesis requires Uge5 alone.
**Conclusion:** Epimerases in *A. fumigatus* play both distinct and overlapping roles in exopolysaccharide synthesis.
**Significance:** Uncovering the biosynthetic pathways of galactosaminogalactan will be crucial in developing therapeutics targeting this exopolysaccharide.

**The cell wall of *Aspergillus fumigatus* contains two galactose-containing polysaccharides, galactomannan and galactosaminogalactan, whose biosynthetic pathways are not well understood. The *A. fumigatus* genome contains three genes encoding putative UDP-glucose 4-epimerases, *uge3*, *uge4*, and *uge5*. We undertook this study to elucidate the function of these epimerases. We found that *uge4* is minimally expressed and is not required for the synthesis of galactose-containing exopolysaccharides or galactose metabolism. Uge5 is the dominant UDP-glucose 4-epimerase in *A. fumigatus* and is essential for normal growth in galactose-based medium. Uge5 is required for synthesis of the galactofuranose (Gal*f*) component of galactomannan and contributes galactose to the synthesis of galactosaminogalactan. Uge3 can mediate production of both UDP-galactose and UDP-*N*-acetylgalactosamine (GalNAc) and is required for the production of galactosaminogalactan but not galactomannan. In the absence of Uge5, Uge3 activity is sufficient for growth on galactose and the synthesis of galactosaminogalactan containing lower levels of galactose but not the synthesis of Gal*f*. A double deletion of *uge5* and *uge3* blocked growth on galactose and synthesis of both Gal*f* and galactosaminogalactan. This study is the first survey of glucose epimerases in *A. fumigatus* and contributes to our understanding of the role of these enzymes in metabolism and cell wall synthesis.**

In immunosuppressed patients, the mold *Aspergillus fumigatus* causes an invasive pulmonary infection that can disseminate hematogenously to the brain and other deep organs. In recent years, the incidence of invasive aspergillosis due to *A. fumigatus* has risen dramatically in patients undergoing immunosuppressive and cytotoxic chemotherapy (1). Although earlier classes of antifungals such as the polyenes and azoles target the fungal plasma membrane, the carbohydrate cell wall is emerging as an effective target for antifungals (2). A better understanding of the composition and biosynthesis of the cell wall and its components will be important in developing new cell wall active antifungals.

The cell wall of *A. fumigatus* is composed of an inner fibrillar layer and an outer amorphous layer (3). The inner layer is composed of a mesh of chitin, β-1,3-glucans, and associated glycoproteins. The outer layer contains α-1,3-glucans, galactomannan, and galactosaminogalactan. Of note, both galactomannan and galactosaminogalactan contain galactose residues, indicating the importance of fungal galactose metabolism in cell wall biosynthesis.

Galactomannan is a branched glycan consisting of an α-linked mannosyl backbone with branches of 4–5 β-linked galactofuranose (Gal*f*)[3] units (4, 5). Gal*f* residues are also found in a variety of other fungal glycoproteins and glycolipids (6, 7). Although the role of galactomannan, and Gal*f*, in virulence

* This work was supported, in whole or in part, by National Institutes of Health Grant R01AI073829. This work was also supported by operating funds from the Canadian Institutes of Health Research.
[1] Supported by a studentship from the Research Institute of the McGill University Health Center.
[2] Supported by a Chercheur-Boursier award from the Fonds de Recherche du Québec-Santé. To whom correspondence should be addressed: Dept. of Microbiology and Immunology, McGill University, 3775 Rue University, Montréal, Québec H3A 2B4, Canada. Tel.: 514-398-1759; Fax: 514-398-7052; E-mail: don.sheppard@mcgill.ca.

[3] The abbreviations used are: Gal*f*, galactofuranose; PDB, Protein Data Bank.

remains unclear (6, 8), immunodetection of Gal*f* antigen by EB-A2 antibody is a widely used diagnostic test for invasive aspergillosis (9–11). Galactomannan biosynthesis has been best studied in the nonpathogenic species *Aspergillus nidulans*. In this species, UDP-glucose is converted to UDP-galactose (UDP-galactopyranose) in the cytoplasm by the UDP-glucose 4-epimerase, UgeA (12). UDP-galactopyranose is in turn modified to UDP-galactofuranose through the activity of the UgmA, an UDP-glucose mutase. UDP-galactofuranose is then transported by the glycosyl transporter, UgtA (13), into the Golgi where the glycosylation of carbohydrates, proteins, and lipids occurs. Although the glycosyltransferases involved in chain formation remain unknown in *Aspergillus*, galactofuranosyltransferases have been studied in bacteria (14–17) and protozoans (18). Although the *A. fumigatus* orthologs of *ugmA* and *ugtA*, termed *ugm1* (*glfA*) and *glfB*, respectively, have been studied and found to have a similar function to their *A. nidulans* orthologs, the *A. fumigatus* ortholog of the *ugeA* epimerase has yet to be identified or characterized (5, 8, 19–21).

Galactosaminogalactan is a recently described galactose-containing cell wall polysaccharide that plays an important role in virulence (22, 23). This glycan mediates adhesion to a variety of host substrates and is immunosuppressive both through directly inducing leukocyte apoptosis, as well as by concealing fungal $\beta$-1,3-glucan from immune recognition by the pattern recognition receptor Dectin-1 (22, 23). Galactosaminogalactan is a linear heteropolysaccharide composed of varying combinations of $\alpha$-1,4-linked galactose and *N*-acetylgalactosamine (GalNAc) (23). The pathways governing synthesis of galactosaminogalactan are largely unknown. Previously, we reported that disruption of *uge3* (Afu3g07910), predicted to encode an UDP-glucose 4-epimerase, resulted in a complete absence of cell wall GalNAc and galactosaminogalactan (22). Gal*f* production and the galactose content of the cell wall were not altered in the Δ*uge3* mutant, suggesting that *uge3* encodes a GlcNAc-GalNAc epimerase. The source of the galactose component of galactosaminogalactan remains unknown.

In addition to *uge3*, the genome of *A. fumigatus* contains genes predicted to encode two other UDP-glucose 4-epimerases, *uge5* (Afu5g10780) and *uge4* (Afu4g14090). Although neither of these epimerases has been studied in *A. fumigatus*, Uge5 is most homologous to the *A. nidulans*, UgeA, which was previously reported to have UDP-glucose 4-epimerase activity (12). Uge4 shares 55% amino acid homology with Uge3 and 60% with a putative epimerase of *Aspergillus niger* (An12g10410), but it has not been studied in either organism. We undertook this study to elucidate the role of these three UDP-glucose 4-epimerases in galactose metabolism and the biosynthesis of *A. fumigatus* cell wall galactose-containing glycans.

## MATERIALS AND METHODS

### Fungal Strains and Growth Conditions

*A. fumigatus* strain Af293 (a generous gift from P. Magee, University of Minnesota, St. Paul, MN) was used as the parent wild-type strain for all molecular manipulations. The Δ*uge3* mutant was described previously (22). Unless otherwise noted, strains were grown and harvested on YPD agar (Fisher) at 37 °C as described previously (24). For growth in liquid medium, Brian medium (23), *Aspergillus* Minimum Medium (25), and RPMI 1640 medium (Wissent) were used as indicated. For agar plates and liquid medium with galactose as the sole source of carbon, Brian agar and liquid medium were modified to include galactose as the only carbon source. For adherence and apoptosis assays, germinated conidia (germlings) were obtained growing either $1 \times 10^5$ or $2 \times 10^5$ conidia in either 24-well plates or 1.5-ml microcentrifuge tubes for 9 h at 37 °C, 5% $CO_2$ incubation in phenol-free RPMI 1640 medium.

### Molecular and Genetic Manipulations

Deletion of *uge4* and *uge5* was performed as described previously (22). Briefly, pAN7.1 plasmid was modified for Gateway® (Invitrogen) use by digestion with restriction enzymes BmgBI or NaeI followed by fusion of an *attR*::*ccdB* target sequence at the site of each digestion using the Gateway® vector conversion system, to generate plasmids pHY and pYG (22). To generate the disruption constructs, ~1 kb of the flanking sequences of *uge5* was amplified by PCR from Af293 genomic DNA using primers U5-1, U5-2, and U5-3, U5-4 to generate fragments FS1 and FS4, respectively. The resulting PCR products were then cloned into pENTR-D -TOPO® entry plasmid. An LR recombination resulted in recombination of pENTR::FS1 with pHY and pENTR::FS4 with pYG, yielding the fusion of each flanking sequence with the *hph* cassette in plasmids pHY and pYG. Finally, the DNA fragments for transformation were generated by PCR, using the primers U5–1,HY with pHY::FS1 and U5–4,YG with pYG::FS4. For Δ*uge4*, the same strategy was used as with Δ*uge5*, except that U4-1, U4-2, U4-3, and U4-4 were used as flanking sequence primers to amplify genomic DNA from Af293. *A. fumigatus* wild-type strain Af293 was then transformed with each pair of disruption cassettes using protoplasting (24). All integrations were confirmed by PCR, and the expected gene expression profile was confirmed by real time RT-PCR for the gene of interest.

For the generation of the Δ*uge3* Δ*uge5* double mutant, plasmid p402 was modified for Gateway® use by digestion with BsaBI or BamHI, followed by a mung bean nuclease treatment in the case of BamHI, and then fusion of an *attR*::*ccdB* target sequence at the site of each digestion to generate plasmids pBL and pLE. An LR recombination allowed recombination of previously produced pENTR::FS1 with pBL and pENTR::FS4 with pLE, resulting in the fusion of each flanking sequence with the *ble* cassette in plasmids pBL and pLE. Finally, the DNA fragments for transformation were generated by PCR, using the primers U5-1,BL with pBL::FS1 and U5-4,LE with pLE::FS4. Protoplasts of the *A. fumigatus* Δ*uge3* mutant strain (22) were then transformed with each DNA fragment, as described previously (22). Transformants were selected on 0.015% phleomycin-enriched plates. Complete deletion of the *uge5* open reading frame was confirmed as described above.

For construction of the Δ*uge5*::*uge5* complemented strain, the plasmid pSK485, bearing a pyrithiamine resistance cassette (26) and obtained from the Fungal Genetics Stock Center (27), was modified by PCR using Sbf-pSK and Asc-pSK primers to add unique SbfI and AscI restriction sites upstream of the *βrec*::*trpA* cassette. The plasmid was then linearized by SbfI and

**TABLE 1**
**List of primers for plasmid construction and gene expression experiments**

| Primer name | Target | Sequence |
|---|---|---|
| U5-1 | uge5 5′-flanking sequence | CACCTTCAAGCGGAACTGGAC |
| U5-2 | uge5 5′-flanking sequence | AAAGGAAGCAGAAGAGCAGAAAGAA |
| U5-3 | uge5 3′-flanking sequence | CACCTGTGAGCGAGAAAGACTGGAAA |
| U5-4 | uge5 3′-flanking sequence | ACATGAAGCAATTAGAGGCAGCA |
| U5-ext 1 | Analysis of uge5 locus | CTTAGTGGACAGCAGACCAGGGG |
| U5-ext 4 | Analysis of uge5 locus | GCGAGAGCCTGACCTATTGCATCT |
| uge5 RT-sense | uge5 cDNA | ATGAGGCCGAGAAGTGGAAC |
| uge5 RT-antisense | uge5 cDNA | CGTGAGAGGCATAGTCGTCA |
| U5-1b | uge5 transcription unit | TACCTGCAGGGTGACATTGATGACGGA |
| U5-5 | uge5 transcription unit | TGGCGCGCCGACAAATATCCAAACGGTA |
| U4-1 | uge4 5′-flanking sequence | CACCGTCGGCTACATTCGT |
| U4-2 | uge4 5′-flanking sequence | AAGGGTTCGCAGTCATCCTC |
| U4-3 | uge4 3′-flanking sequence | CACCAATCTCACAGCTAACG |
| U4-4 | uge4 3′-flanking sequence | CGCAGACATACCACTTCTTG |
| U4-ext 1 | Analysis of uge5 locus | GGCCCCAAAATCAGGAGT |
| U4-ext 4 | Analysis of uge5 locus | ATCGCATCTACGCCATGATT |
| uge4 RT-sense | uge4 cDNA | CATCCACACCCCTCTGAAGT |
| uge4 RT-antisense | uge4 cDNA | CGGACGAGGAGAAGATGAAG |
| U3-start ORF | $His_6$-Uge3 production | CACCATGGACAGCTACCAGCAATC |
| U3-end ORF | $His_6$-Uge3 production | AAGGGACATGCGACAACATC |
| HY | hph | CAACCACGGCCTCCAGAAGAAGA |
| YG | hph | GCGAGAGCCTGACCTATTGCATCT |
| tef1-RT sense | tef1 | CCATGTGTGTCGAGTCCTTC |
| tef1-RT antisense | tef1 | GAACGTACAGCAACAGTCTGG |
| Sbf-pSK | pSK485 modification | AGCTTCCTGCAGGTAAATCAAAAGAATAGACCGAGATA |
| Asc-pSK | pSK485 modification | TGGCGCGCCTAAGGGATTTTGCCGATTTC |
| Uge5-RFP forward | Campoli *et al.* (31) | CATCACCCCATGGATATGTCTGCTGGTTCAGTT |
| Uge5-RFP-reverse | Campoli *et al.* (31) | GGAGGAGGCCATGATCTTCTTGAGCTGTTCCAG |
| Uge3-gfp forward | Choe *et al.* (29) | AGACATCACCCCATGGATGGACAGCTACCAGCA |
| Uge3-gfp reverse | Choe *et al.* (29) | CTCACCATCGCGGCCGCAGTAGATAACCCACTGA |

AscI digestion. A 2.9-kb DNA fragment, corresponding to the restriction site SbfI, 1.2 kb of the *uge5* promoter, the entire *uge5* ORF, 0.8 kb of the *uge5* terminator and the restriction sites AscI, was amplified by PCR using Af293 DNA as a template and the primers U5-1b and U5-5. The resulting PCR product was cloned into the linearized pSK485 plasmid via the Infusion® cloning reaction, following the manufacturer's instructions. The resulting pSK485::*uge5* plasmid was linearized at the unique DraI site, located upstream of the *uge5* partial promoter, and was used to transform protoplasts of the Δ*uge5* strain. Transformants were selected on 0.1 μg/ml pyrithiamine-enriched plates, and *uge5* expression was confirmed by RT-PCR.

To generate the *uge3-gfp* construct, the *uge3* gene was amplified by PCR using primers uge3-gfp forward and uge3-gfp reverse. This PCR fragment was then cloned into the pGFP plasmid, as described previously, and digested with NcoI and NotI (28, 29). The resulting plasmid, designated p*uge3*-GFP, was used to transform wild-type *A. fumigatus* Af293 as described previously (30). Transformants were selected by phleomycin resistance, and *uge3-gfp* expression was verified using confocal microscopy (IX81, Olympus), excitation wavelength 495 nm and emission wavelength 519 nm.

To generate the *uge5-rfp* construct, *uge5* was amplified by PCR using primers uge5-rfp forward and uge5-rfp reverse. This fragment was then cloned in-frame with mRFP1 in the pRFP-HYG plasmid using EcoRV (31). The resulting plasmid pRFP-Uge5-HYG was used to transform wild-type *A. fumigatus* Af293. Transformants were selected using hygromycin, and *uge5-rfp* expression was verified using confocal microscopy (IX81, Olympus), excitation 543 nm and emission wavelength 563 nm.

For $His_6$-Uge3, the ORF of *uge3* was produced by PCR with an additional CACC at the 5′ end, using the primers U3-start ORF, U3-end ORF, and the Af293 genomic DNA as template. The resulting PCR product was then cloned into pENTR-D-TOPO® entry plasmid. An LR recombination allowed the recombination of pENTR::U3-ORF with pDest17®, a plasmid engineered to produce $His_6$ proteins with a high rate in proper *Escherichia coli* strains. The resulting pDest17::*uge3* plasmid was transformed in *E. coli* BL21 DE3 strain. All primer sequences are listed in Table 1.

### *Real Time RT-PCR*

Expression of the genes of interest was quantified by relative real time RT-PCR analysis as described previously (32). The primers used for each of the genes are shown in Table 1 or in Gravelat *et al.* (22). First strand synthesis was performed from total RNA with the QuantiTec reverse transcription kit (Qiagen) using random primers. Real time PCR was then performed using an ABI 7000 thermocycler (Applied Biosystems). Amplification products were detected with the Maxima® SYBR Green qPCR system (Fermentas). Fungal gene expression was normalized to *A. fumigatus tef1* expression. To verify the absence of genomic DNA contamination, negative controls were used for each gene set in which reverse transcriptase was omitted from the mix.

### *Localization Studies*

Conidia from *uge3-gfp, uge5-rfp,* or *A. fumigatus* Af293 strains were grown for 9 h at 37 °C on coverslips in a 24-well polystyrene plate in RPMI 1640 medium without phenol. Young hyphae were washed in PBS, stained with Draq® nuclear staining at 1:100 dilution (Cell Signaling, Inc), mounted in Slow Fade® Gold Antifade (Invitrogen), and imaged under a confocal microscope (IX81, Olympus) at excitation 495, 543, and 633 nm, respectively.

### *Cell Culture Assays*

Type II pneumocyte cell line CCL-185 (lung epithelial cells A549) and murine bone marrow-derived dendritic cells were cultured as described previously (22).

*Aspergillus* adherence to A549 cells was determined by co-incubating germlings of the strain of interest on a monolayer of A549 cells for 30–45 min, as described previously (24). To determine induction of apoptosis via caspase-3 activity, germlings of each strain were co-incubated with bone marrow-derived dendritic cells at a multiplicity of infection of 10:1 for 3 h. Caspase-3 activity was measured using EnzChek® Caspase-3 assay kit following the manufacturer's instructions (Invitrogen). Samples containing fungus or bone marrow-derived dendritic cells alone were included as controls.

### *Polysaccharide Analysis*

Galactosaminogalactan and Gal*f* productions were assayed as described previously, with minor modifications (22, 23). Briefly, $4 \times 10^6$ conidia were grown in modified Brian medium for 72 h. Culture supernatants were filtered, and extracellular galactosaminogalactan or galactomannan was precipitated by 2.5 or 4.0 volumes of ethanol, respectively. Galactosaminogalactan composition was determined by gas chromatography after hydrolysis, reduction, and peracetylation with meso-inositol as internal standard. Total neutral hexoses were quantified by the phenol sulfuric assay. Gal*f* quantification was assayed by enzyme immunoassay using the Platelia® *Aspergillus* kit (Bio-Rad), following the manufacturer's instructions. For quantification of $\beta$-1,3-glucan exposure, $1 \times 10^5$ conidia were grown in Brian medium for 12 h in a 96-well opaque bottom plate (Nunclon, Inc.), fixed in 4% paraformaldehyde, and then labeled with 10 $\mu$g/ml Fc-Dectin-1 (a generous gift from Dr. G. D. Brown, University of Aberdeen, Aberdeen, UK), followed by FITC-labeled AffiniPure F(ab′) fragment donkey anti-human IgG, FCy fragment-specific (Jackson ImmunoResearch). Fluorescence was measured at 495 nm excitation and 515 nm emission using Spectramax® fluorescence microplate reader (Molecular Devices, Inc.). The biofilm adherence assay and scanning electron microscopy were performed as described previously (22, 24).

### *His-tagged Uge3 Extraction and Purification*

Protein expression of $His_6$-Uge3 was performed in *E. coli* BL21(DES) in autoinduction medium supplemented with 100 $\mu$g/ml ampicillin (33). Cells were grown for 20–24 h at 28 °C and harvested by centrifugation. Pellets were flash-frozen and then lysed and filtered through a 0.2-$\mu$m nylon membrane filter and incubated for 1.5 h in $Ni^{2+}$-agarose beads (Qiagen). After successive washing with increasing imidazole concentrations, bound $His_6$-Uge3 was eluted with 250 mM imidazole. Fractions containing $His_6$-Uge3 determined by SDS-PAGE Coomassie Blue staining were pooled, concentrated, and quantified with either Bradford assay or NanoDrop®. Alternatively, after cell lysis, $His_6$-Uge3 was purified through metal affinity chromatography on a POROS-MC20 perfusion chromatography column with $Ni^{2+}$ as chelating metal. Elution fractions were pooled and further purified on a preparative scale high resolution Superdex-200 gel filtration column. Purification of $His_6$-Uge3 was validated though Western blotting using HRP-tagged anti-$His_6$ (Abcam) and protein mass spectrometry. Enzymes were stored at −20 °C in PBS supplemented with 25% glycerol and 0.5 mM DTT.

### *Enzyme Activity Assays*

*Product Formation*—Evolution of product was detected using NMR by incubating 5 $\mu$g of $His_6$-Uge3 with 1 mM of either UDP-glucose or UDP-GlcNAc (Sigma) in a reaction mix of 250 $\mu$l for 1 h at 37 °C. No co-factor was added because preliminary experiments did not show any changes to the reaction rate by adding co-factors such as $NAD^+$, $Mg^{2+}$, or $Ca^{2+}$ (data not shown), as similarly reported in other epimerases (34–36). All reagents were in $D_2O$ (Calbiochem), and spectra were recorded at 25 °C with acetone internal reference (2.23 ppm) using standard pulse COSY, TOCSY (mixing time 120 ms), and $^1H,^{31}P$ HMQC. NMR experiments were performed on Varian INOVA® 500 MHz spectrometer with a 3-mm gradient probe. Spectra assignment was performed using Bruker Topspin Version 3.1 program for spectra visualization.

*Enzyme Kinetics*—The rates of product formation, linearity, and kinetics studies were performed using Beckman gold capillary electrophoresis with a 57-cm bare silica capillary, and 32 Karat software application, as described previously (37). Concentrations of substrates, ranging from 0.2 to 5.0 mM for UDP-GlcNAc and from 0.01 to 1 mM for UDP-galactose, were used to obtain product formation data in the presence of 0.25 or 0.53 pmol of Uge3 for each substrate. For kinetics study, enzyme with varying concentrations of substrates in a 10-$\mu$l reaction volume of 0.1 M Tris/HCl buffer at pH 8.0 was incubated at 37 °C for the specified amount of time, quenched by boiling at 95 °C for 5 min, and immediately stored at −80 °C. Prior to incubation, all reagents and enzymes were kept at 4 °C. Electropherogram peaks were integrated using 32 Karat software application to estimate substrate conversion. $V_{max}$ values of the reactions were calculated by taking the reciprocal of the *Y*-intercept, and $K_m$ values of the reactions were calculated by taking the slope over the *Y*-intercept (data not shown).

### *Bioinformatics Analysis*

*Annotation and Homology*—UDP-glucose 4-epimerase genes and their respective amino acid sequences were retrieved from the *Aspergillus* Genome Database (38). The amino acid sequences of each of the candidate epimerases were analyzed using Eukaryotic Linear Motif (39), ConSurf (40), Conserved Domain Database (41), and HHpred (42), including SCOP domains. Clusters and protein families by domain predictions were cross-referenced using InterPro (43, 44) and Pfam (45). Furthermore, each of the *Aspergillus* epimerases were matched with the closest protein entry available in the Protein Data Bank (46) and further annotated.

*Homology Structural Modeling*—The amino acid sequence of Uge3 was aligned with human GalE PDB code 1HZJ (47), *Trypanosoma brucei* GalE PDB code 1GY8 (48), or *Pseudomonas aeruginosa* WbpP PDB code 1SB8 (49) using ClustalW (50). Aligned Uge3 sequences were then modeled against each of the template structures using Modeler Version 9.11 (51). Resulting

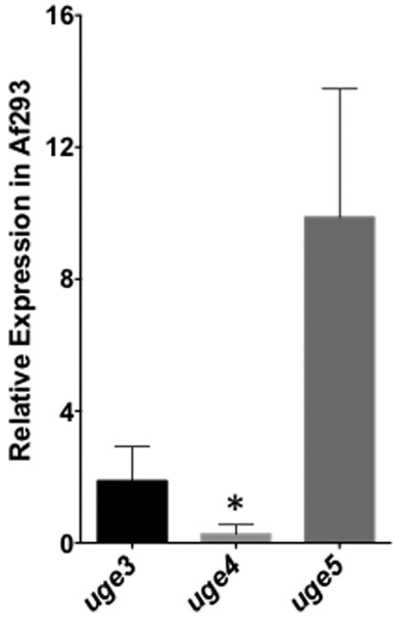


FIGURE 1. ***uge5* gene is the most highly expressed of the three epimerase genes in *A. fumigatus*, whereas *uge4* mRNA expression is barely detectable.** Strain Af293 was grown in Brian medium for 18 h, and the levels of *uge3, uge4,* and *uge5* mRNA were measured by real time RT-PCR. *, indicates significantly different expression as compared with *tef1* reference gene (22).

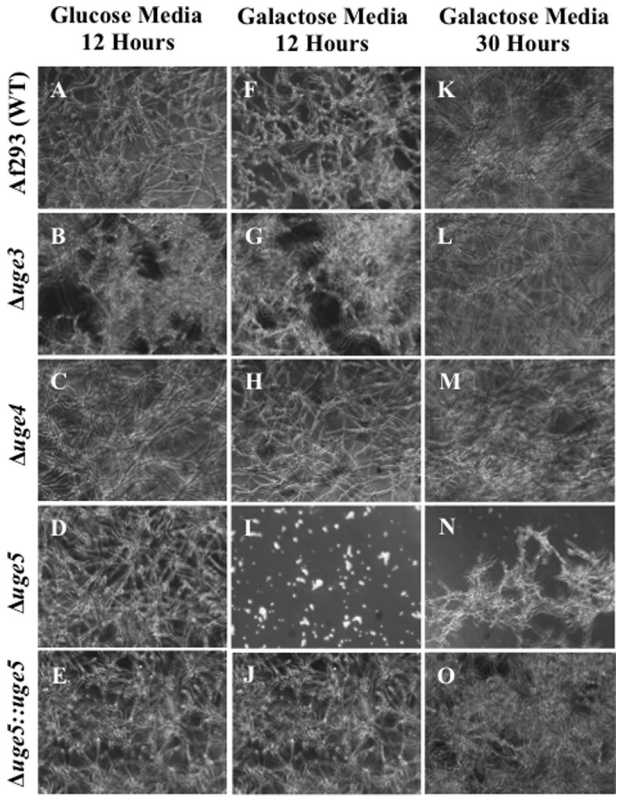


FIGURE 2. **Deletion of *uge5* results in a partial galactose auxotrophy.** The indicated strains were grown for the indicated time periods in Brian medium with either glucose (*A–E*) or galactose (*F–O*) as the sole carbon source. Bright field images at a magnification of ×200 are shown.

models were verified using Pairwise Structure Alignment (46). MacPyMOL Version 1.3 (academic license, Schrodinger LLC) was used to align respective structures and identify and analyze key residues in the catalytic site.

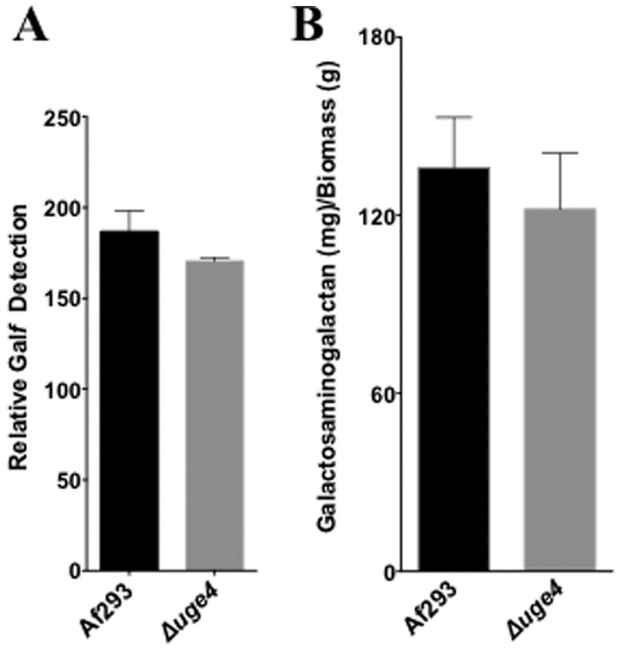


FIGURE 3. **Deletion of *uge4* does not alter galactosaminogalactan or Galf production.** *A,* relative Galf detection by ELISA (EB-A2) in culture supernatant of Af293 or Δ*uge4* mutant after 72 h growth of indicated strains in Brian medium. *B,* galactosaminogalactan production by biomass from culture supernatant of Af293 or Δ*uge4* mutant after 72 h growth of the indicated strains in Brian medium.

### *Statistical Analysis*

All charts and graphs were produced and analyzed using Prism 6 (GraphPad software). All tables were created using MS Excel (Microsoft Inc.).

## RESULTS

*Uge5 Is the Most Highly Expressed Epimerase Gene in A. fumigatus and Is Required for Normal Galactose Metabolism*—We first performed expression analysis of the three epimerase genes in wild-type *A. fumigatus* grown in Brian medium (Fig. 1). Of the three epimerase-encoding genes, *uge5* was the most highly expressed, at a level more than 5-fold higher than that of *uge3*. Expression of *uge4* was minimal, approaching the limits of detection by real time RT-PCR. We therefore hypothesized that Uge5 likely plays an important role in galactose metabolism and cell wall glycan synthesis.

To test the role of each of these three epimerases in galactose metabolism, Δ*uge4* and Δ*uge5 A. fumigatus* deletion mutants were constructed. The ability of these mutants to utilize glucose and galactose was compared with the previously constructed Δ*uge3* mutant and wild-type *A. fumigatus* strains (22). All three mutant strains exhibited wild-type growth on medium with glucose as the sole carbon source (Fig. 2, *A–E*). Similarly, both the Δ*uge3* and Δ*uge4* mutants grew normally on medium with galactose as a sole carbon source (Fig. 2, *F–H*). Deletion of *uge5* resulted in a marked impairment of growth in medium containing galactose as a sole carbon source (Fig. 2, *I–J*), consistent with the findings reported with the deletion of *ugeA,* the *A. nidulans* ortholog of *uge5* (12). However, unlike the *A. nidulans* Δ*ugeA* mutant, the Δ*uge5* mutant was not completely blocked in hyphal growth under these conditions and was able to grow

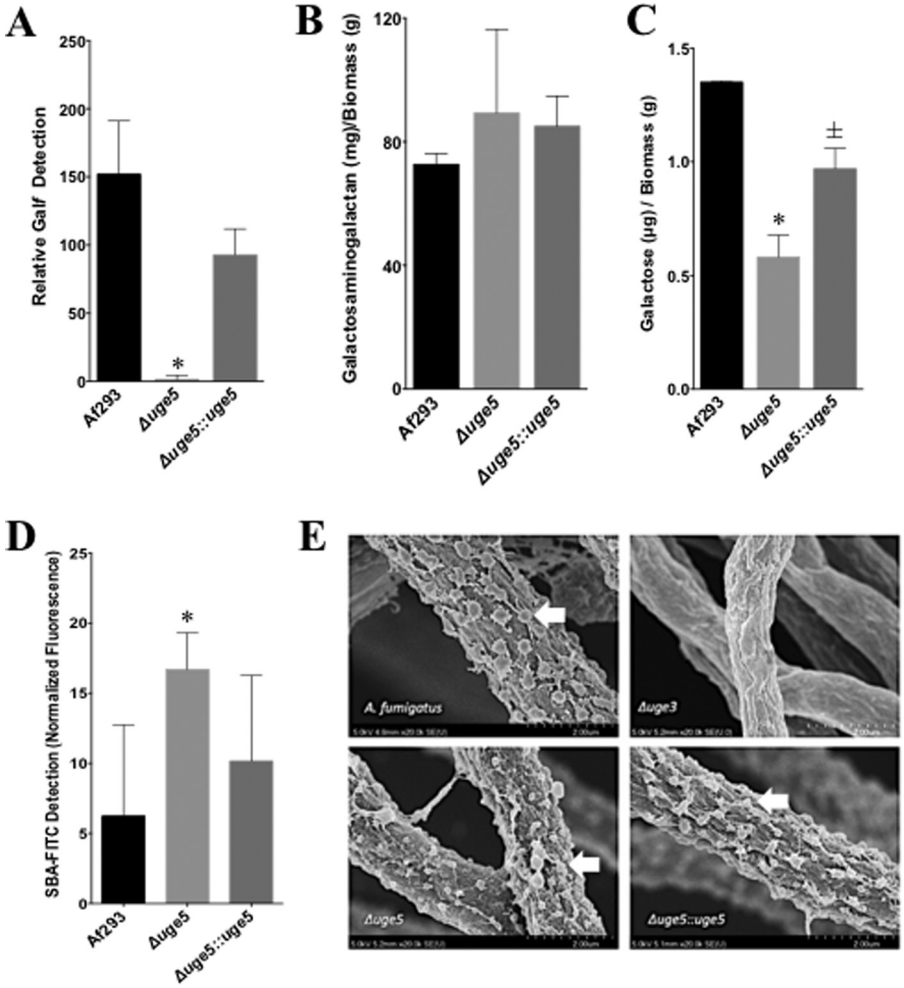


FIGURE 4. **Deletion of *uge5* blocks Gal*f* synthesis and results in production of galactosaminogalactan with a reduced galactose content.** *A,* Gal*f* content of culture supernatants as determined by ELISA. *B,* galactosaminogalactan content of culture supernatants, normalized to mycelia biomass. *C,* galactose content of galactosaminogalactan from the indicated strains as detected by gas chromatography followed by hexose and hexosamine quantification. *D,* FITC-tagged GalNAc-specific soybean agglutinin (*SBA*) lectin binding on 12-h, Brian medium-grown hyphae of indicated strains. Total fluorescence was measured with Spectramax® fluorescence microplate reader. *E,* scanning electron micrograph of hyphae of indicated strains after 24 h of growth at 37 °C, 5% $CO_2$ in phenol-free RPMI 1640. Hyphae were fixed, sequentially dehydrated in ethanol, dried in $CO_2$, coated in Pd-Au, and imaged under scanning electron microscope (Hitachi). *Arrows* indicate surface decorations associated with galactosaminogalactan production. *, significant reduction compared with Af293 wild-type, analysis of variance with pairwise comparison $p < 0.05$. ±, not statistically significant compared with Af293 but statistically significant compared with the Δ*uge5* mutant, $p < 0.05$. *A–C,* indicated strains were grown for 72 h in Brian medium.

and form hyphae after 30 h of growth in galactose (Fig. 2*N*). Collectively, these results suggest that *A. fumigatus* differs from *A. nidulans* in that whereas *uge5* is the major epimerase responsible for the interconversion of UDP-galactose and UDP-glucose, other pathways or enzymes in *A. fumigatus* can mediate galactose metabolism in the absence of Uge5.

*Deletion of Uge5 Blocks Galf Synthesis and Results in the Production of Galactosaminogalactan with Reduced Galactose Content*—To test the contribution of each of the three epimerases to the synthesis of galactose-containing glycans, we measured the production of galactosaminogalactan and Gal*f* by each of these mutant strains. We previously found that deletion of *uge3* results in a complete block in galactosaminogalactan synthesis but had no effect on Gal*f* synthesis (22). Deletion of *uge4* had no effect on Gal*f* detection or galactosaminogalactan production (Fig. 3, *A* and *B*). Consistent with reports of *ugeA* deletion in *A. nidulans* (12), deletion of *uge5* resulted in the absence of detectable Gal*f* antigen and, by extension, the absence of galactomannan (Fig. 4*A*). Unexpectedly, however, multiple assays demonstrated that deletion of *uge5* did not block galactosaminogalactan synthesis. Scanning electron microscopy of the Δ*uge5* mutant identified normal production of the cell wall decorations that have been associated with galactosaminogalactan production (Fig. 4*E*) (22), and levels of total galactosaminogalactan produced by the Δ*uge5* mutant were slightly higher than those seen with the wild type, although this was not statistically significant (Fig. 4*B*). Compositional analysis of galactosaminogalactan from the Δ*uge5* mutant revealed a significant reduction in the galactose content of this heteropolysaccharide (Fig. 4*C*). This decrease in galactose was not associated with an increase in other hexose such as glucose or mannose (data not shown). The Δ*uge5* mutant also exhibited increased staining with the GalNAc-specific soybean agglutinin lectin (Fig. 4*D*), consistent with the production of GalNAc-rich, galactose-poor galactosaminogalactan. Collectively, these data suggest that although Uge5 activity is required for UDP-Gal*f* syn-

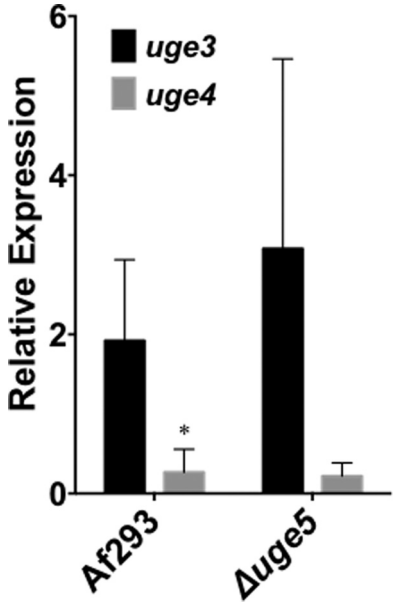


FIGURE 5. **Deletion of *uge5* is not associated with significant up-regulation of expression of *uge3* or *uge4*.** The indicated strains were grown in Brian medium for 18 h, and the levels of *uge3* (*black bar*) and *uge4* (*gray bar*) mRNA from indicated strains were measured by real time RT-PCR. *, significant difference between *uge3* and *uge4* expression in the indicated strain as compared with *tef1* reference gene, factorial analysis of variance with pairwise comparison, $p < 0.05$.

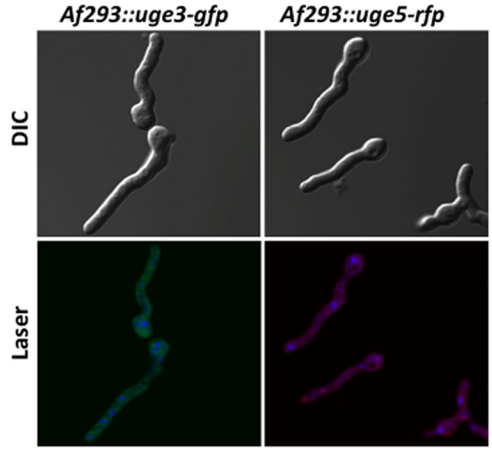


FIGURE 6. **Uge3 and Uge5 are cytoplasmic.** Af293 strains expressing *uge3-gfp* or *uge5-rfp* were grown in Brian medium for 12 h and imaged by confocal microscopy. For nuclear staining, Draq5® stain was used, and pseudocolor blue was red fluorescent protein at 543 nm, and Draq5® at 633 nm.

thesis for the production of galactomannan, other enzymes or pathways can also contribute UDP-galactose to the synthesis of galactosaminogalactan in the absence of Uge5 activity.

*Uge3 Activity May Compensate for the Lack of Uge5*—The Δ*uge5* mutant was able to utilize galactose as a carbon source and produced galactosaminogalactan that still contained galactose. These data suggest that this strain retained some glucose/galactose epimerase activity, possibly mediated by Uge4 or Uge3. Although disruption of *uge4* had no effect on galactose metabolism, galactosaminogalactan or Gal*f* production, *uge4* was only expressed at very low levels in the wild-type strain of *A. fumigatus*, and therefore, it could be up-regulated in the absence of Uge5. To test for compensatory up-regulation of *uge4* in the absence of Uge5, we performed real time RT-PCR analysis of *uge4* expression in this mutant. The expression of *uge4* remained minimally detectable in the Δ*uge5* mutant under galactosaminogalactan-inducing conditions (Fig. 5). In contrast, not only was *uge3* expression detectable in wild-type *A. fumigatus*, but a trend toward increased *uge3* expression was observed in the absence of Uge5 (Fig. 5). Collectively, these data suggest that Uge3 may have dual substrate specificity and can mediate the interconversion of both UDP-glucose to UDP-galactose and UDP-GlcNAc to UDP-GalNAc. Consistent with this model, expression of *uge3-gfp* or *uge5-rfp* in wild-type *A. fumigatus* demonstrated that both of these epimerases are located in the cytoplasm (Fig. 6), and thus could provide galactose to the same downstream glycosyltransferases or mediate conversion of galactose to glucose for metabolic use.

*Homology Modeling Suggests Uge3 Is a Group 2 Epimerase with Dual Substrate Specificity*—To examine the possibility that Uge3 could exhibit dual substrate binding and catalysis, the structure of Uge3 was compared with those of other UDP-glucose 4-epimerases by homology modeling. UDP-glucose 4-epimerases are composed of three groups based on substrate specificity (52) as follows: group 1 enzymes have specificity for hexoses, group 2 for both hexoses and hexosamines, and group 3 for hexosamines. Uge3 was therefore modeled using *T. brucei* tGalE (PDB code 1GY8) as a group 1 template, human hGalE (PDB code 1HZJ) as a group 2 template, and *P. aeruginosa* WbpP (PDB code 1SB8) as a group 3 template. The N-terminal portion of Uge3 encoding a predicted signal peptide was omitted from modeling. Inspection of amino acid residues in the catalytic sites of the Uge3 model and templates revealed similarities and differences in the predicted substrate-binding pocket region that may provide further insights to Uge3's catalytic activity. Similar to tGalE, hGalE, and WbpP, the SYK triad required for catalytic activity is conserved in the Uge3 model ($Ser^{191}$, $Tyr^{238}$, and $Lys^{242}$) (49, 53). Previously, six amino acid residues forming the hexagonal substrate-binding pocket were identified to be important in enzymatic function (49, 52). Identification of the corresponding residues on Uge3 revealed that these residues are not only present in Uge3, but that they are identical to hGalE, which belongs to the bifunctional group 2 (Table 2). In fact, these six residues in Uge3 and hGalE align almost in a complete overlap around the cofactor and substrate (Fig. 7). Thus, the *in silico* analysis suggests that Uge3 is structurally more closely related to the group 2 epimerase hGALE and may play a role in the interconversion of both UDP-Glc/UDP-Gal, as well as UDP-GlcNAc/UDP-GalNAc.

*Uge3 Is a Dual Substrate Epimerase That Can Utilize Both UDP-glucose and UDP-N-acetylglucosamine as Substrates*—To test if Uge3 has dual substrate activity, recombinant Uge3 was produced (Fig. 8, *A* and *B*) and its enzymatic activity measured. Using $^1$H NMR, product formation of both UDP-galactose and UDP-GalNAc was detected in the presence of Uge3 when either UDP-glucose or UDP-GlcNAc was provided as a substrate, respectively (Fig. 8, *C* and *D*, and Table 3). To obtain better resolution of the peaks, COSY and TOCSY two-dimensional $^1$H NMR experiments were performed and demonstrated that the cross-peaks of coupled protons show both substrate and product chemical shifts in the respective reaction mixes (data not

**TABLE 2**

**Alignment of the six amino acid residues within the catalytic fold of Uge3, hGalE, tGalE, and WbpP shows highest alignment between Uge3 and hGalE**

Six amino acid residues in the catalytic pocket were identified on the Uge3 model. These residues were then compared with those in hGalE, tGalE, and WbpP. Visualization was performed using MacPyMOL Version 1.3.

| Species | Enzyme | Residues | | | | | | Group |
|---|---|---|---|---|---|---|---|---|
| *A. fumigatus* | Uge3 | $Lys^{151}$ | $Ser^{191}$ | $Tyr^{238}$ | $Asn^{268}$ | $Asn^{288}$ | $Cys^{391}$ | 2 |
| *H. sapiens* | hGalE | $Lys^{92}$ | $Ser^{132}$ | $Tyr^{157}$ | $Asn^{187}$ | $Asn^{206}$ | $Cys^{307}$ | 2 |
| *T. brucei* | tGalE | $Leu^{102}$ | $Ser^{142}$ | $Tyr^{173}$ | $Asn^{202}$ | $His^{202}$ | $Leu^{342}$ | 1 |
| *P. aeruginosa* | WbpP | $Gly^{102}$ | $Ser^{142}$ | $Tyr^{166}$ | $Asn^{195}$ | $Ala^{209}$ | $Ser^{306}$ | 3 |

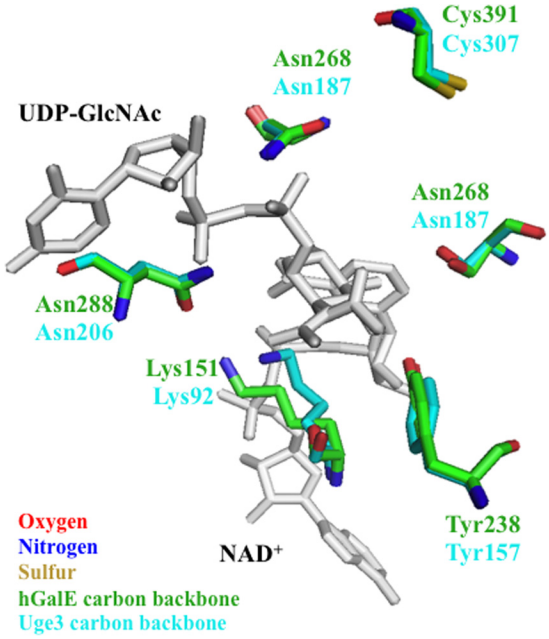


FIGURE 7. **Substrate-binding pocket of Uge3 model aligns with hGalE.** The hexagonal substrate-binding pocket of Uge3 model (*green*) was aligned to hGalE (*cyan*), with the six residues required for catalytic activity annotated. For Uge3 homology modeling, the N-terminal nonalignment regions were discarded, and resulting aligned sequences were modeled using Modeler Version 9.11. Bound UDP-GalNAc and $NAD^+$ are indicated in *gray* at *top and bottom*, respectively.

shown). To further validate that the products retained their UDP moieties and were not derivatives or different species of galactose or GalNAc, $^{31}P$ NMR was performed and detected the same phosphorus chemical shifts in both respective substrate and product proton peaks (data not shown). Uge3 activity was further characterized using capillary electrophoresis. At steady-state equilibrium, Uge3 converted 30% of UDP-GlcNAc to UDP-GalNAc and 15% of UDP-glucose to UDP-galactose (Fig. 8*E*). The range of reaction time that resulted in linearity of product formation of less than 10% for Michaelis-Menten analysis was determined to be between 0 and 30 min for both substrates (data not shown). Conversion from UDP-GlcNAc to UDP-GalNAc had $K_m$ of 3.2 mM and $V_{max}$ of 417 pmol/min (data not shown). Epimerization from UDP-glucose to UDP-galactose could not be quantified due to a strong reverse reaction; however, conversion of UDP-galactose to UDP-glucose had a $K_m$ of 0.9 mM and $V_{max}$ of 146 pmol/min (data not shown). Collectively, these results support the hypothesis that the galactose component of galactosaminogalactan in the Δ*uge5* mutant strain likely originates from activity of Uge3.

*Mutant Deficient in Both Uge3 and Uge5 Is Completely Auxotrophic for Galactose and Produces No Galactomannan or Galactosaminogalactan*—To verify that Uge3 activity is responsible for the residual galactose metabolism and galactose content of galactosaminogalactan in the Δ*uge5* mutant strain, we constructed a mutant deficient in both Uge3 and Uge5. The Δ*uge3*Δ*uge5* double mutant was unable to grow in medium containing galactose as the sole carbon source (Fig. 9, *A* and *B*). Furthermore, the Δ*uge3*Δ*uge5* double mutant was found to have undetectable levels of both Gal*f* and galactosaminogalactan (Fig. 9, *C* and *D*). Collectively these data confirm that Uge3 and Uge5 are the only functional UDP-glucose/galactose epimerases in *A. fumigatus*.

*Reducing the Galactose Component of Galactosaminogalactan Does Not Impair Its Function*—To assess whether the galactose-poor galactosaminogalactan produced by the Δ*uge5* mutant is altered in function, we characterized the effects of *uge5* deletion on the reported functions of galactosaminogalactan (22, 23). Deletion of *uge5* did not alter biofilm adherence to the polystyrene surface (Fig. 10*A*). Furthermore, Δ*uge5* mutant displayed slightly increased adherence to A549 epithelial cells as compared with wild-type *A. fumigatus* and the *uge5*-complemented strain, possibly reflecting the slight increase in total galactosaminogalactan production noted in this strain (Fig. 10*B*). Similarly the reduced galactose content of galactosaminogalactan did not impair β-(1,3)-glucan masking, as there was no difference between these three strains in the immunodetection of β-(1,3)-glucan by recombinant Fc-dectin-1 (Fig. 10*C*). Finally, because leukocyte apoptosis has been reported as a mechanism of galactosaminogalactan immunosuppression (23), the ability of the Δ*uge5* mutant to induce apoptosis of bone marrow-derived dendritic cells was quantified by measuring cellular caspase-3 activity. No difference in the induction of apoptosis by the Δ*uge5* mutant as compared with wild-type *A. fumigatus* (Fig. 10*D*) was observed. Collectively, lowering the galactose content of galactosaminogalactan did not seem to significantly impair adherence, β-(1,3)-glucan masking, or the induction of apoptosis by this glycan.

## DISCUSSION

The results of our studies highlight important differences in galactose metabolism, glycan synthesis, and epimerase function between *A. fumigatus* and *A. nidulans*. Although deletion of *ugeA* in *A. nidulans* resulted in a strain that was completely auxotrophic for galactose, the *A. fumigatus* Δ*uge5* mutant exhibited only a partial growth defect in galactose-containing medium. In light of our findings that Uge3 has dual substrate specificity and that other putative epimerases are silent in the Δ*uge5* mutant, it is likely that Uge3 mediates the interconver-

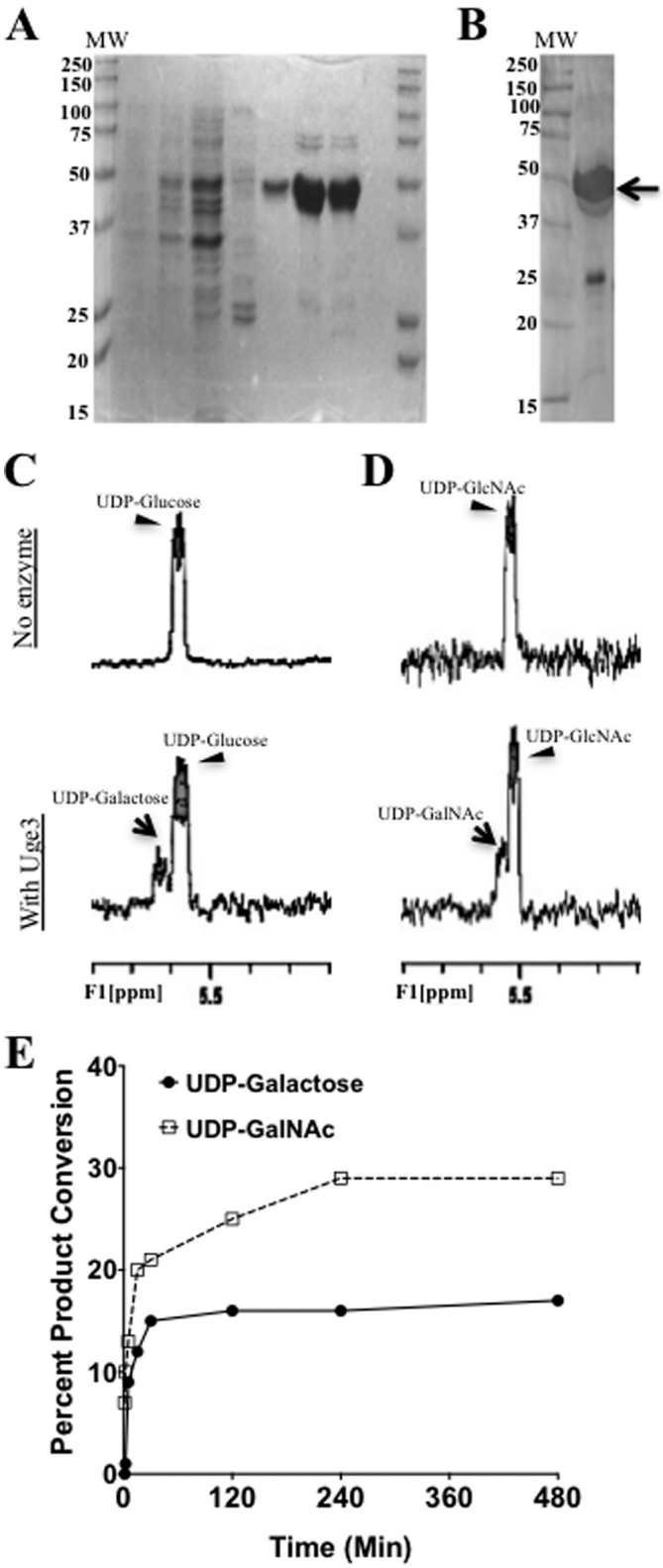


FIGURE 8. **Uge3 exhibits bifunctional UDP-Glc/UDP-Gal and UDP-GlcNAc/UDP-GalNAc epimerase activity.** *A,* SDS-PAGE of lysate and purified $His_6$-Uge3 stained with Commassie Blue from $His_6$-Uge3 expressing BL21(DE) *E. coli* strain. *Lanes* are as follows: noninduced cells; cells grown in auto-induction medium; crude lysate; wash fraction eluted using 20 mM imidazole; and four fractions of $His_6$-Uge3 eluted with 250 mM imidazole. *B,* Western blot of purified lysates for detection of $His_6$-Uge3 using HRP-tagged anti-$His_6$ antibody. *Arrow* indicates expected band for $His_6$-Uge3. *C* and *D,* $^1$H NMR spectra were measured in a reaction mix containing either UDP-glucose (*C*) or UDP-GlcNAc (*D*) in phosphate buffer, in the presence or absence of Uge3. For all NMR experiments, products were detected after 1 h of co-incubation of Uge3 and respective substrates at 37 °C using Varian 500 MHz NMR spectroscopy. *E,* rate of product formation was measured using capillary electrophoresis over time in a reaction mix containing 20 pmol of Uge3 and 0.1 mM of either UDP-glucose or UDP-GlcNAc as substrate. Reactions took place at 37 °C in a total volume of 10 $\mu$l. Products were detected at 254 nm (UV) measuring UDP-moiety endogenous fluorescence. UDP-linked sugars were separated by borate adduct formation.

**TABLE 3**
**$^1$H NMR chemical shift and constant for product and substrate**

| Unit | H/C 1 | H/C 2 | H/C 3 | H/C 4 | H/C 5 | H/C 6 |
|---|---|---|---|---|---|---|
| UDP-Glc | 5.6 | 3.53 | 3.78 | 3.47 | 3.9 | 3.78; 3.86 |
| $J_{Hn,Hn+1}$ | 3 | 9 | 9 | 9 | | |
| UDP-Gal | 5.64 | 3.8 | 3.92 | 4.03 | 4.17 | 3.74; 3.77 |
| $J_{Hn,Hn+1}$ | 3 | 9 | <2 | <2 | | |
| UDP-GlcNAc | 5.51 | 3.99 | 3.81 | 3.55 | 3.93 | 3.87; 3.93 |
| $J_{Hn,Hn+1}$ | 3 | 9 | 9 | 9 | | |
| UDP-GalNAc | 5.55 | 4.26 | 3.97 | 4.05 | 4.19 | 3.76; 3.78 |
| $J_{Hn,Hn+1}$ | 3 | 9 | <2 | <2 | | |

sion between UDP-glucose and UDP-galactose in the absence of Uge5 (Fig. 11). Although the genome of *A. nidulans* contains *ugeB*, an ortholog of *uge3*, this gene has been reported to be silent (55) and as a result likely does not contribute to UDP-galactose/UDP-glucose interconversion in this species.

Disruption of *uge5* was associated with normal to increased galactosaminogalactan production and adherence to host cells. These data are consistent with those from mutations in other components of the galactomannan biosynthetic pathways. For example, deletion of *ugm1* in *A. fumigatus* resulted not only in an absence of galactomannan but also an increase in galactosaminogalactan synthesis and biofilm adherence (6). Although galactosaminogalactan production has not been studied in *A. nidulans*, it was reported that the deletion of *ugmA* and *ugeA* was associated with an increase in adherence (55), suggesting a similar phenomenon may also occur in this organism. One possibility is that impaired galactomannan synthesis results in accumulation of precursors that are then redirected to the galactosaminogalactan pathway. If this is true, then such substrate flux must occur at the level of UDP-glucose or earlier given that the Δ*uge5* mutant retained the ability to produce galactosaminogalactan. Alternatively, the increase in galactosaminogalactan could reflect activation of a regulatory response to alterations in cell wall integrity as has been observed to occur with other mutations or perturbing agents that alter cell wall composition (56–59).

It is surprising that, in the absence of Uge5, UDP-galactose production by Uge3 was sufficient to permit production of galactosaminogalactan but not Gal*f*. Although compartmental sequestration of the UDP-galactose produced by these two epimerases could account for this observation, our localization studies suggest that both enzymes are cytoplasmic. Alternatively, differences in the transport of UDP-galactose or the substrate affinity of downstream enzymes specific for each of the two pathways could mediate this preferential funneling of UDP-galactose into galactosaminogalactan synthesis. It is not known if either epimerase complexes with other elements in their respective biosynthetic pathways; however, this explanation could account for differences in accessibility of UDP-galactose between pathways. Finally, there may be different regu-

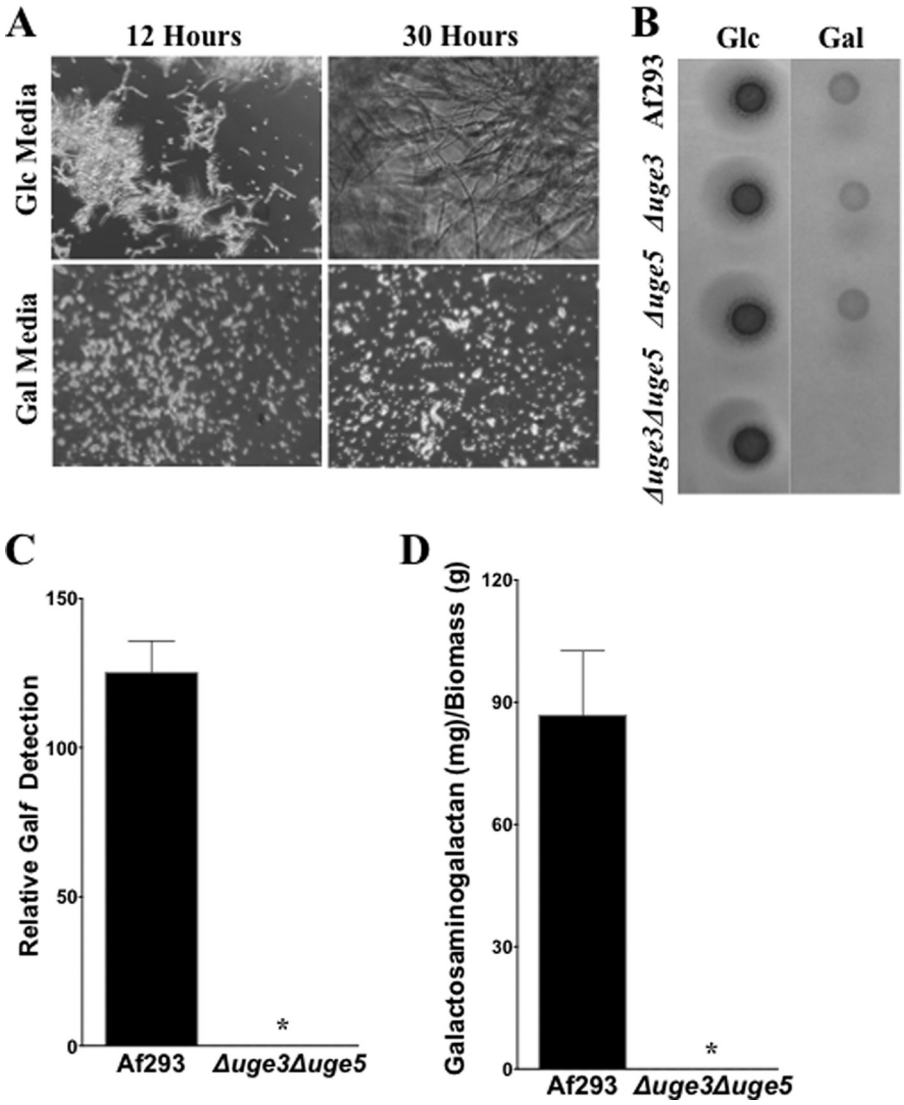


FIGURE 9. **Deletion of *uge3* and *uge5* renders the resulting Δ*uge3*Δ*uge5* double mutant deficient in Gal*f* and galactosaminogalactan.** *A,* indicated strains were grown for the indicated time periods in Brian medium using either glucose or galactose as the sole carbon source. Brightfield images at a magnification of 200x are shown. Glucose is abbreviated as Glc, and galactose as Gal. *B,* indicated strains were grown for 2 days on either glucose or galactose based Brian medium agar plates. *C,* relative Gal*f* detection by ELISA in culture supernatant after 72 h growth in Brian medium of the indicated strains. *D,* galactosaminogalactan production after 72 h growth in Brian medium of the indicated strains. *, significant reduction compared with Af293 wild type and analysis of variance with pairwise comparison, $p < 0.05$.

latory controls at various levels of gene expression and protein synthesis of other pathway components. Although a deficiency in galactosaminogalactan is not lethal, it renders the strain non-adherent, which is not the case for galactomannan deficiency (5, 6, 8, 12, 22). Thus, in the absence of a specific requirement for galactomannan, it is possible that the fungus preferentially diverts its resources to preserve galactosaminogalactan synthesis for adherence to surfaces or biofilm homeostasis. Testing of these hypotheses will require identification of other elements of the galactosaminogalactan biosynthetic pathways, an area under active research by our group.

We initially hypothesized that enzymes upstream of Uge3 or Uge5 in the Leloir pathway, such as galactokinase or UDP-galactose-1-phosphate uridylyltransferase, may contribute to the residual galactose found in the Δ*uge5* mutant. Although much of the Leloir pathway is uncharacterized in *A. fumigatus*, it is well characterized in *A. nidulans*. In this species, deletion of galactokinase gene *galE* or UDP-galactose-1-phosphate uridylyltransferase *galD* results in mutants that are viable, albeit with partial growth defects, in a galactose-based carbon source (60). However, the complete lack of growth of the Δ*uge3*Δ*uge5* double mutant in galactose-based medium strongly suggests that these epimerases are solely responsible for galactose metabolism under the conditions studied in this report, and other salvage enzymes are insufficient to provide adequate glucose from galactose under the conditions of growth that we tested.

Our findings demonstrate that Uge3 is dispensable for galactose metabolism and Gal*f* synthesis. This observation is likely due, at least in part, to the much lower expression levels of *uge3* as compared with *uge5*. Indeed, it is possible that interconversion of UDP-galactose and UDP-glucose by Uge3 does not occur in the presence of physiologic levels of Uge5 and is only unmasked upon Uge5 deletion. Interestingly, we found that, *in vitro*, Uge3 produced twice as much UDP-GalNAc compared

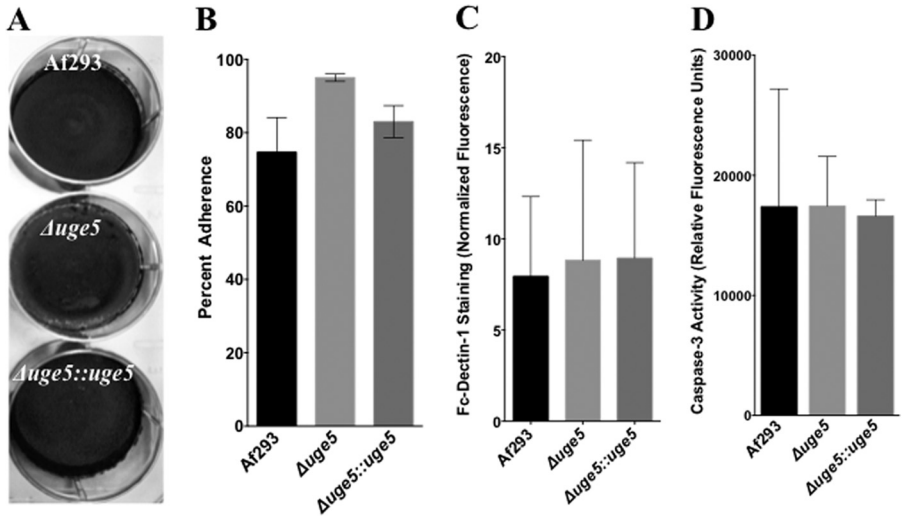


FIGURE 10. **Galactose-poor Δ*uge5* galactosaminogalactan retains normal virulence-associated functions.** *A,* biofilm adherence of indicated strains after 24 h of growth on polystyrene plates, after several washes, and visualized by staining with crystal violet. *B,* adherence of germinated hyphae of the indicated strains to A549 epithelial cells after 30 min. *C,* detection of Fc-dectin-1 binding using immune staining. Conidia from respective strains were grown for 12 h in Brian medium, fixed, blocked, stained with Fc-dectin-1, and FITC-labeled F(ab) fragment, and total fluorescence was measured with Spectramax® fluorescence microplate reader. *D,* induction of bone marrow-derived dendritic cell apoptosis as determined by caspase-3 activity. Conidia from indicated strains were grown for 9 h in RPMI 1640 medium and then co-incubated with mouse bone marrow-derived dendritic cells at a multiplicity of infection of 10:1. Caspase-3 activity was measured by commercial assay following the manufacturer's instructions (Invitrogen).

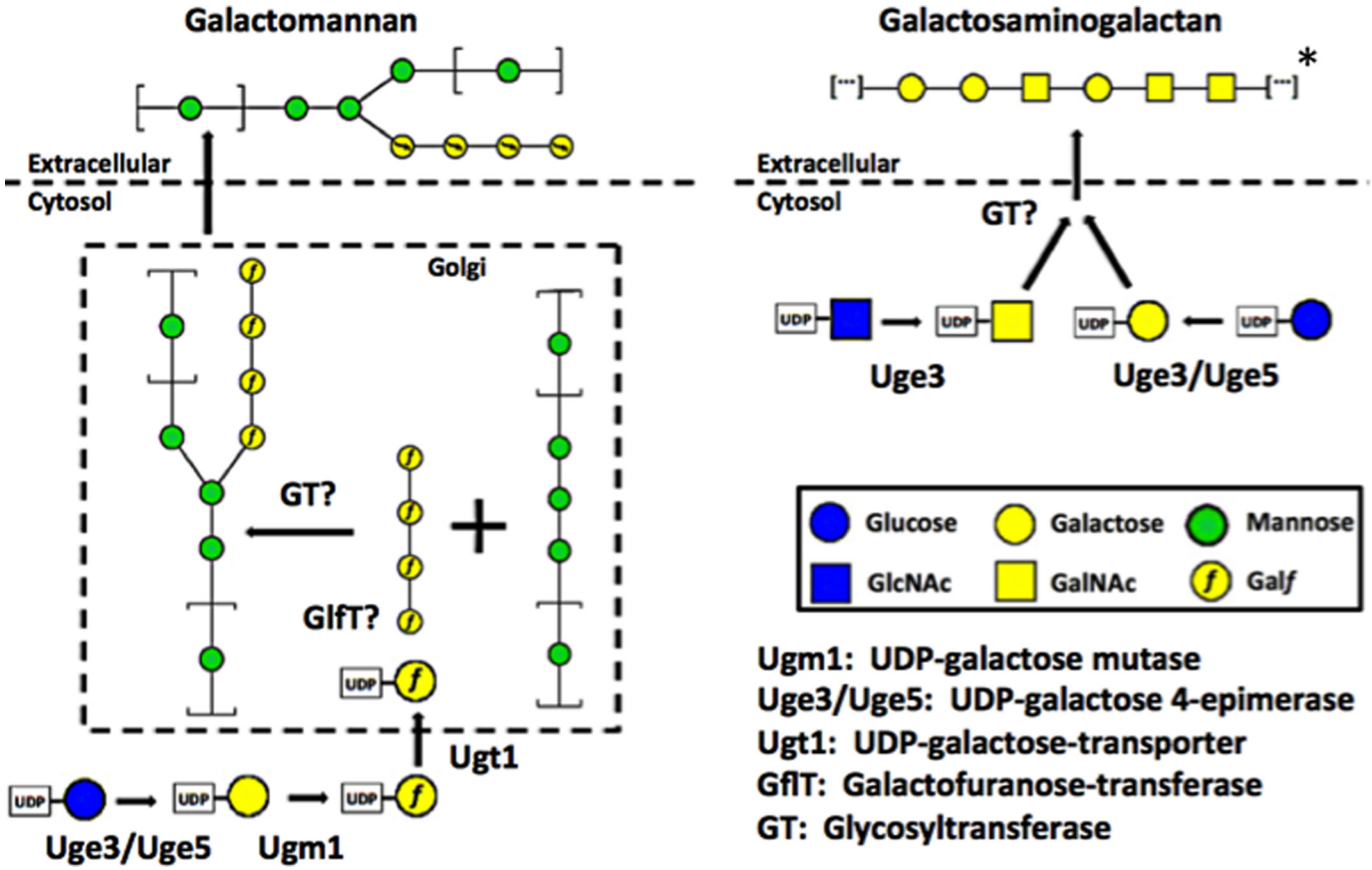


FIGURE 11. **Schematic of galactosaminogalactan and galactomannan pathways.** Pathway diagrams showing common and distinct components in the biosynthesis of galactosaminogalactan and galactomannan. For Gal*f* symbol representation, the "*f*" has been inserted to the galactose pyranose symbol. All other symbols follow common nomenclature convention (54). *, note that the depiction of galactosaminogalactan structure is representative of multiple potential combinations of galactose and GalNAc residues.

with UDP-galactose from respective substrates at steady-state equilibrium, thus suggesting a possible preference toward *N*-acetylated hexosamines as substrates. Nonetheless, this redundancy in UDP-galactose and UDP-glucose interconversion by two epimerases suggests that interconversion of hexoses may be more critical to *A. fumigatus* than the interconver-

sion of UDP-GlcNAc-UDP-GalNAc, which is mediated by Uge3 alone (22). Indeed, sugar epimerase have important functions outside of cell wall polysaccharide synthesis, such as metabolism. Redundancy in hexose interconversion would ensure that the organism can adapt to different carbon sources and maintain glycolysis and generate derivatives required for other cellular activities (12, 13, 61–63). In contrast, GalNAc seems to be required by *A. fumigatus* primarily for the synthesis of galactosaminogalactan and is not required for normal growth (22). The need for redundant hexose epimerase activity is unlikely related to galactosaminogalactan synthesis, because production of galactose-poor galactosaminogalactan by the Δ*uge5* mutant did not impair adherence, biofilm formation, or other virulence associated properties. Indeed, our studies failed to identify a functional role for the galactose component of galactosaminogalactan and suggest that the adherence, apoptosis-inducing, and pathogen-associated molecular pattern-masking phenotypes of galactosaminogalactan are mediated by the GalNAc fraction of this glycan. One possibility is that altering the galactose content of galactosaminogalactan may provide a mechanism for the organism to modulate galactosaminogalactan activity through secondarily changing the relative GalNAc content of the resulting glycan. We are currently investigating the effects of lowering the GalNAc content of galactosaminogalactan to better understand the mechanism of action of galactosaminogalactan in these phenotypes.

Although we found three genes annotated as UDP-glucose 4-epimerases in *A. fumigatus*, only *uge3* and *uge5* seem to be active. One explanation could be that the *in silico* annotation is not correct and that, in fact, *uge4* is not a UDP-glucose 4-epimerase. However, based on the close homology of *uge4* to the other two epimerases, and the fact that all important domains are predicted with high certainty to be intact in the *uge4* sequence, it is likely that *uge4* is a UDP-glucose 4-epimerase. It is possible that *uge4* is expressed under conditions that were not tested; however, an alternative explanation is that *uge4* is a product of gene duplication that could have served a purpose earlier in evolution but has now become silenced. Similar silent gene duplications have been reported in other cell wall-related genes in *A. fumigatus* (64, 65). Interestingly, silencing of epimerases in *Aspergillus* species may play a role in virulence because in the nonpathogenic species *A. nidulans, ugeB,* the ortholog of *A. fumigatus uge3*, has been reported to be silent (55).

This study broadens our understanding of *Aspergillus* epimerases and their role in metabolism and carbohydrate synthesis, and it also begins to identify some of the critical steps in the biosynthesis of galactosaminogalactan. These results suggest a model of galactose-containing cell wall polysaccharide synthesis in which Uge5 activity alone mediates production of UDP-galactose as a precursor to Gal*f* and subsequent galactomannan synthesis. Conversely, Uge3 activity is required for the synthesis of UDP-GalNAc for the production of galactosaminogalactan, and both epimerases can contribute to the pool of UDP-galactose used in the synthesis of galactosaminogalactan. Furthermore, Uge5 is responsible for the majority of the epimerase activity within the Leloir pathway, as deletion of *uge5*, but not *uge3*, was associated with a defect in growth on galactose-containing medium. A deeper understanding of the biochemical pathways underlying galactose metabolism and the biosynthesis of cell wall glycans in this pathogenic fungus may provide the basis for the development of future antifungal therapies.

*Acknowledgments—We are thankful to Marianne Ngure and Moheshwarnath Issur for their guidance on protein purification.*

## REFERENCES


1. Garcia-Vidal, C., Upton, A., Kirby, K. A., and Marr, K. A. (2008) Epidemiology of invasive mold infections in allogeneic stem cell transplant recipients: biological risk factors for infection according to time after transplantation. *Clin. Infect. Dis.* **47,** 1041–1050
2. Ostrosky-Zeichner, L., Casadevall, A., Galgiani, J. N., Odds, F. C., and Rex, J. H. (2010) An insight into the antifungal pipeline: selected new molecules and beyond. *Nat. Rev. Drug Discov.* **9,** 719–727
3. Latgé, J.-P. (2010) Tasting the fungal cell wall. *Cell. Microbiol.* **12,** 863–872
4. Latge, J. P. (2009) Galactofuranose containing molecules in *Aspergillus fumigatus*. *Med. Mycol.* **47,** S104–S109
5. Latgé, J. P., Kobayashi, H., Debeaupuis, J. P., Diaquin, M., Sarfati, J., Wieruszeski, J. M., Parra, E., Bouchara, J. P., and Fournet, B. (1994) Chemical and immunological characterization of the extracellular galactomannan of *Aspergillus fumigatus*. *Infect. Immun.* **62,** 5424–5433
6. Lamarre, C., Beau, R., Balloy, V., Fontaine, T., Wong Sak Hoi, J., Guadagnini, S., Berkova, N., Chignard, M., Beauvais, A., and Latgé, J.-P. (2009) Galactofuranose attenuates cellular adhesion of *Aspergillus fumigatus*. *Cell. Microbiol.* **11,** 1612–1623
7. Tefsen, B., Ram, A. F., van Die, I., and Routier, F. H. (2012) Galactofuranose in eukaryotes: aspects of biosynthesis and functional impact. *Glycobiology* **22,** 456–469
8. Schmalhorst, P. S., Krappmann, S., Vervecken, W., Rohde, M., Müller, M., Braus, G. H., Contreras, R., Braun, A., Bakker, H., and Routier, F. H. (2008) Contribution of galactofuranose to the virulence of the opportunistic pathogen *Aspergillus fumigatus*. *Eukaryot. Cell* **7,** 1268–1277
9. Luong, M.-L., Filion, C., Labbé, A.-C., Roy, J., Pépin, J., Cadrin-Tourigny, J., Carignan, S., Sheppard, D. C., and Laverdière, M. (2010) Clinical utility and prognostic value of bronchoalveolar lavage galactomannan in patients with hematologic malignancies. *Diagn. Microbiol. Infect. Dis.* **68,** 132–139
10. Walsh, T. J., Anaissie, E. J., Denning, D. W., Herbrecht, R., Kontoyiannis, D. P., Marr, K. A., Morrison, V. A., Segal, B. H., Steinbach, W. J., Stevens, D. A., van Burik, J.-A., Wingard, J. R., Patterson, T. F., Infectious Diseases Society of America (2008) Treatment of aspergillosis: clinical practice guidelines of the Infectious Diseases Society of America. *Clin. Infect. Dis.* **46,** 327–360
11. Stynen, D., Sarfati, J., Goris, A., Prévost, M. C., Lesourd, M., Kamphuis, H., Darras, V., and Latgé, J. P. (1992) Rat monoclonal antibodies against *Aspergillus galactomannan*. *Infect. Immun.* **60,** 2237–2245
12. El-Ganiny, A. M., Sheoran, I., Sanders, D. A., and Kaminskyj, S. G. (2010) *Aspergillus nidulans* UDP-glucose 4-epimerase UgeA has multiple roles in wall architecture, hyphal morphogenesis, and asexual development. *Fungal Genet. Biol.* **47,** 629–635
13. Afroz, S., El-Ganiny, A. M., Sanders, D. A., and Kaminskyj, S. G. (2011) Roles of the *Aspergillus nidulans* UDP-galactofuranose transporter, UgtA in hyphal morphogenesis, cell wall architecture, conidiation, and drug sensitivity. *Fungal Genet. Biol.* **48,** 896–903
14. Kremer, L., Dover, L. G., Morehouse, C., Hitchin, P., Everett, M., Morris, H. R., Dell, A., Brennan, P. J., McNeil, M. R., Flaherty, C., Duncan, K., and Besra, G. S. (2001) Galactan biosynthesis in *Mycobacterium tuberculosis*. Identification of a bifunctional UDP-galactofuranosyltransferase. *J. Biol. Chem.* **276,** 26430–26440
15. Guan, S., Clarke, A. J., and Whitfield, C. (2001) Functional analysis of the galactosyltransferases required for biosynthesis of D-galactan I, a component of the lipopolysaccharide O1 antigen of *Klebsiella pneumoniae*. *J. Bacteriol.* **183,** 3318–3327
16. Mikusová, K., Belánová, M., Korduláková, J., Honda, K., McNeil, M. R., Mahapatra, S., Crick, D. C., and Brennan, P. J. (2006) Identification of a

novel galactosyltransferase involved in biosynthesis of the mycobacterial cell wall. *J. Bacteriol.* **188,** 6592–6598
17. Wing, C., Errey, J. C., Mukhopadhyay, B., Blanchard, J. S., and Field, R. A. (2006) Expression and initial characterization of WbbI, a putative D-Gal*f*: α-D-Glcβ-1,6-galactofuranosyltransferase from *Escherichia coli* K-12. *Org. Biomol. Chem.* **4,** 3945–3950
18. Stoco, P. H., Aresi, C., Lückemeyer, D. D., Sperandio, M. M., Sincero, T. C., Steindel, M., Miletti, L. C., and Grisard, E. C. (2012) *Trypanosoma rangeli* expresses a β-galactofuranosyltransferase. *Exp. Parasitol.* **130,** 246–252
19. Bakker, H., Kleczka, B., Gerardy-Schahn, R., and Routier, F. H. (2005) Identification and partial characterization of two eukaryotic UDP-galactopyranose mutases. *Biol. Chem.* **386,** 657–661
20. Engel, J., Schmalhorst, P. S., Dörk-Bousset, T., Ferrières, V., and Routier, F. H. (2009) A single UDP-galactofuranose transporter is required for galactofuranosylation in *Aspergillus fumigatus*. *J. Biol. Chem.* **284,** 33859–33868
21. Oppenheimer, M., Poulin, M. B., Lowary, T. L., Helm, R. F., and Sobrado, P. (2010) Characterization of recombinant UDP-galactopyranose mutase from *Aspergillus fumigatus*. *Arch. Biochem. Biophys.* **502,** 31–38
22. Gravelat, F. N., Beauvais, A., Liu, H., Lee, M. J., Snarr, B. D., Chen, D., Xu, W., Kravtsov, I., Hoareau, C. M., Vanier, G., Urb, M., Campoli, P., Al Abdallah, Q., Lehoux, M., Chabot, J. C., Ouimet, M.-C., Baptista, S. D., Fritz, J. H., Nierman, W. C., Latgé, J. P., Mitchell, A. P., Filler, S. G., Fontaine, T., and Sheppard, D. C. (2013) *Aspergillus* galactosaminogalactan mediates adherence to host constituents and conceals hyphal β-glucan from the immune system. *PLoS Pathog.* 10.1371/journal.ppat.1003575
23. Fontaine, T., Delangle, A., Simenel, C., Coddeville, B., van Vliet, S. J., van Kooyk, Y., Bozza, S., Moretti, S., Schwarz, F., Trichot, C., Aebi, M., Delepierre, M., Elbim, C., Romani, L., and Latge, J. P. (2011) Galactosaminogalactan, a new immunosuppressive polysaccharide of *Aspergillus fumigatus*. *PLoS Pathog.* 10.1371/journal.ppat.1002372
24. Gravelat, F. N., Ejzykowicz, D. E., Chiang, L. Y., Chabot, J. C., Urb, M., Macdonald, K. D., al-Bader, N., Filler, S. G., and Sheppard, D. C. (2010) *Aspergillus fumigatus* MedA governs adherence, host cell interactions, and virulence. *Cell. Microbiol.* **12,** 473–488
25. Gravelat, F. N., Askew, D. S., and Sheppard, D. C. (2012) Targeted gene deletion in *Aspergillus fumigatus* using the hygromycin-resistance split-marker approach. *Methods Mol. Biol.* **845,** 119–130
26. Hartmann, T., Dümig, M., Jaber, B. M., Szewczyk, E., Olbermann, P., Morschhäuser, J., and Krappmann, S. (2010) Validation of a self-excising marker in the human pathogen *Aspergillus fumigatus* by employing the β-rec/six site-specific recombination system. *Appl. Environ. Microbiol.* **76,** 6313–6317
27. McCluskey, K., Wiest, A., and Plamann, M. (2010) The Fungal Genetics Stock Center: a repository for 50 years of fungal genetics research. *J. Biosci.* **35,** 119–126
28. Al Abdallah, Q., Choe, S. I., Campoli, P., Baptista, S., Gravelat, F. N., Lee, M. J., and Sheppard, D. C. (2012) A conserved C-terminal domain of the *Aspergillus fumigatus* developmental regulator MedA is required for nuclear localization, adhesion and virulence. *PLoS One,* 10.1371/journal.pone.0049959
29. Choe, S. I., Gravelat, F. N., Al Abdallah, Q., Lee, M. J., Gibbs, B. F., and Sheppard, D. C. (2012) Role of *Aspergillus niger* acrA in arsenic resistance and its use as the basis for an arsenic biosensor. *Appl. Environ. Microbiol.* **78,** 3855–3863
30. Twumasi-Boateng, K., Yu, Y., Chen, D., Gravelat, F. N., Nierman, W. C., and Sheppard, D. C. (2009) Transcriptional profiling identifies a role for BrlA in the response to nitrogen depletion and for StuA in the regulation of secondary metabolite clusters in *Aspergillus fumigatus*. *Eukaryot. Cell* **8,** 104–115
31. Campoli, P., Perlin, D. S., Kristof, A. S., White, T. C., Filler, S. G., and Sheppard, D. C. (2013) Pharmacokinetics of posaconazole within epithelial cells and fungi: Insights into potential mechanisms of action during treatment and prophylaxis. *J. Infect. Dis.* 10.1093/infdis/jit358
32. Gravelat, F. N., Doedt, T., Chiang, L. Y., Liu, H., Filler, S. G., Patterson, T. F., and Sheppard, D. C. (2008) *In vivo* analysis of *Aspergillus fumigatus* developmental gene expression determined by real-time reverse transcription-PCR. *Infect. Immun.* **76,** 3632–3639
33. Studier, F. W. (2005) Protein production by auto-induction in high density shaking cultures. *Protein Expr. Purif.* **41,** 207–234
34. Gu, X., Lee, S. G., and Bar-Peled, M. (2011) Biosynthesis of UDP-xylose and UDP-arabinose in *Sinorhizobium meliloti* 1021: first characterization of a bacterial UDP-xylose synthase, and UDP-xylose 4-epimerase. *Microbiology* **157,** 260–269
35. Creuzenet, C., Belanger, M., Wakarchuk, W. W., and Lam, J. S. (2000) Expression, purification, and biochemical characterization of WbpP, a new UDP-GlcNAc C4 epimerase from *Pseudomonas aeruginosa* serotype O6. *J. Biol. Chem.* **275,** 19060–19067
36. Johnson, A. E., and Tanner, M. E. (1998) Epimerization via carbon-carbon bond cleavage. L- Ribulose-5-phosphate 4-epimerase as a masked class II aldolase. *Biochemistry* **37,** 5746–5754
37. McCallum, M., Shaw, G. S., and Creuzenet, C. (2011) Characterization of the dehydratase WcbK and the reductase WcaG involved in GDP-6-deoxy-manno-heptose biosynthesis in *Campylobacter jejuni*. *Biochem. J.* **439,** 235–248
38. Arnaud, M. B., Cerqueira, G. C., Inglis, D. O., Skrzypek, M. S., Binkley, J., Chibucos, M. C., Crabtree, J., Howarth, C., Orvis, J., Shah, P., Wymore, F., Binkley, G., Miyasato, S. R., Simison, M., Sherlock, G., and Wortman, J. R. (2012) The *Aspergillus* Genome Database (AspGD): recent developments in comprehensive multispecies curation, comparative genomics and community resources. *Nucleic Acids Res.* **40,** D653–D659
39. Dinkel, H., Michael, S., Weatheritt, R. J., Davey, N. E., Van Roey, K., Altenberg, B., Toedt, G., Uyar, B., Seiler, M., Budd, A., Jödicke, L., Dammert, M. A., Schroeter, C., Hammer, M., Schmidt, T., Jehl, P., McGuigan, C., Dymecka, M., Chica, C., Luck, K., Via, A., Chatr-Aryamontri, A., Haslam, N., Grebnev, G., Edwards, R. J., Steinmetz, M. O., Meiselbach, H., Diella, F., and Gibson, T. J. (2012) ELM–the database of eukaryotic linear motifs. *Nucleic Acids Res.* **40,** D242–D251
40. Celniker, G., Nimrod, G., Ashkenazy, H., Glaser, F., Martz, E., Mayrose, I., Pupko, T., and Ben-Tal, N. (2013) ConSurf: using evolutionary data to raise testable hypotheses about protein function. *Isr. J. Chem.* **53,** 199–206
41. Marchler-Bauer, A., Lu, S., Anderson, J. B., Chitsaz, F., Derbyshire, M. K., DeWeese-Scott, C., Fong, J. H., Geer, L. Y., Geer, R. C., Gonzales, N. R., Gwadz, M., Hurwitz, D. I., Jackson, J. D., Ke, Z., Lanczycki, C. J., Lu, F., Marchler, G. H., Mullokandov, M., Omelchenko, M. V., Robertson, C. L., Song, J. S., Thanki, N., Yamashita, R. A., Zhang, D., Zhang, N., Zheng, C., and Bryant, S. H. (2011) CDD: a Conserved Domain Database for the functional annotation of proteins. *Nucleic Acids Res.* **39,** D225–D229
42. Biegert, A., Mayer, C., Remmert, M., Söding, J., and Lupas, A. N. (2006) The MPI Bioinformatics toolkit for protein sequence analysis. *Nucleic Acids Res.* **34,** W335–W339
43. Apweiler, R., Attwood, T. K., Bairoch, A., Bateman, A., Birney, E., Biswas, M., Bucher, P., Cerutti, L., Corpet, F., Croning, M. D., Durbin, R., Falquet, L., Fleischmann, W., Gouzy, J., Hermjakob, H., Hulo, N., Jonassen, I., Kahn, D., Kanapin, A., Karavidopoulou, Y., Lopez, R., Marx, B., Mulder, N. J., Oinn, T. M., Pagni, M., Servant, F., Sigrist, C. J., and Zdobnov, E. M. (2001) The InterPro database, an integrated documentation resource for protein families, domains and functional sites. *Nucleic Acids Res.* **29,** 37–40
44. Hunter, S., Jones, P., Mitchell, A., Apweiler, R., Attwood, T. K., Bateman, A., Bernard, T., Binns, D., Bork, P., Burge, S., de Castro, E., Coggill, P., Corbett, M., Das, U., Daugherty, L., Duquenne, L., Finn, R. D., Fraser, M., Gough, J., Haft, D., Hulo, N., Kahn, D., Kelly, E., Letunic, I., Lonsdale, D., Lopez, R., Madera, M., Maslen, J., McAnulla, C., McDowall, J., McMenamin, C., Mi, H., Mutowo-Muellenet, P., Mulder, N., Natale, D., Orengo, C., Pesseat, S., Punta, M., Quinn, A. F., Rivoire, C., Sangrador-Vegas, A., Selengut, J. D., Sigrist, C. J., Scheremetjew, M., Tate, J., Thimmajanarthanan, M., Thomas, P. D., Wu, C. H., Yeats, C., and Yong, S. Y. (2012) InterPro in 2011: new developments in the family and domain prediction database. *Nucleic Acids Res.* **40,** D306–D312
45. Punta, M., Coggill, P. C., Eberhardt, R. Y., Mistry, J., Tate, J., Boursnell, C., Pang, N., Forslund, K., Ceric, G., Clements, J., Heger, A., Holm, L., Sonnhammer, E. L., Eddy, S. R., Bateman, A., and Finn, R. D. (2012) The Pfam protein families database. *Nucleic Acids Res.* **40,** D290–D301
46. Bernstein, F. C., Koetzle, T. F., Williams, G. J., Meyer, E. F., Jr., Brice, M. D., Rodgers, J. R., Kennard, O., Shimanouchi, T., and Tasumi, M. (1977) The

Protein Data Bank: a computer-based archival file for macromolecular structures. *J. Mol. Biol.* **112,** 535–542
47. Thoden, J. B., Wohlers, T. M., Fridovich-Keil, J. L., and Holden, H. M. (2001) Human UDP-galactose 4-epimerase. Accommodation of UDP-*N*-acetylglucosamine within the active site. *J. Biol. Chem.* **276,** 15131–15136
48. Shaw, M. P., Bond, C. S., Roper, J. R., Gourley, D. G., Ferguson, M. A., and Hunter, W. N. (2003) High-resolution crystal structure of *Trypanosoma brucei* UDP-galactose 4′-epimerase: a potential target for structure-based development of novel trypanocides. *Mol. Biochem. Parasitol.* **126,** 173–180
49. Ishiyama, N., Creuzenet, C., Lam, J. S., and Berghuis, A. M. (2004) Crystal structure of WbpP, a genuine UDP-*N*-acetylglucosamine 4-epimerase from *Pseudomonas aeruginosa*: substrate specificity in UDP-hexose 4-epimerases. *J. Biol. Chem.* **279,** 22635–22642
50. Larkin, M. A., Blackshields, G., Brown, N. P., Chenna, R., McGettigan, P. A., McWilliam, H., Valentin, F., Wallace, I. M., Wilm, A., Lopez, R., Thompson, J. D., Gibson, T. J., and Higgins, D. G. (2007) Clustal W and Clustal X version 2.0. *Bioinformatics* **23,** 2947–2948
51. Eswar, N., John, B., Mirkovic, N., Fiser, A., Ilyin, V. A., Pieper, U., Stuart, A. C., Marti-Renom, M. A., Madhusudhan, M. S., Yerkovich, B., and Sali, A. (2003) Tools for comparative protein structure modeling and analysis. *Nucleic Acids Res.* **31,** 3375–3380
52. Demendi, M., Ishiyama, N., Lam, J. S., Berghuis, A. M., and Creuzenet, C. (2005) Toward a better understanding of the substrate specificity of the UDP-*N*-acetylglucosamine C4 epimerase WbpP. *Biochem. J.* **389,** 173–180
53. Jörnvall, H., Persson, B., Krook, M., Atrian, S., Gonzàlez-Duarte, R., Jeffery, J., and Ghosh, D. (1995) Short-chain dehydrogenases/reductases (SDR). *Biochemistry* **34,** 6003–6013
54. Varki, A., Cummings, R. D., Esko, J. D., Freeze, H. H., Stanley, P., Marth, J. D., Bertozzi, C. R., Hart, G. W., and Etzler, M. E. (2009) Symbol nomenclature for glycan representation. *Proteomics* **9,** 5398–5399
55. Paul, B. C., El-Ganiny, A. M., Abbas, M., Kaminskyj, S. G., and Dahms, T. E. (2011) Quantifying the importance of galactofuranose in *Aspergillus nidulans* hyphal wall surface organization by atomic force microscopy. *Eukaryot. Cell* **10,** 646–653
56. Henry, C., Latgé, J.-P., and Beauvais, A. (2012) β1,3-Glucans are dispensable in *Aspergillus fumigatus*. *Eukaryot. Cell* **11,** 26–29
57. Verwer, P. E., van Duijn, M. L., Tavakol, M., Bakker-Woudenberg, I. A., and van de Sande, W. W. (2012) Reshuffling of *Aspergillus fumigatus* cell wall components chitin and β-glucan under the influence of caspofungin or nikkomycin Z alone or in combination. *Antimicrob. Agents Chemother.* **56,** 1595–1598
58. Fortwendel, J. R., Juvvadi, P. R., Pinchai, N., Perfect, B. Z., Alspaugh, J. A., Perfect, J. R., and Steinbach, W. J. (2009) Differential effects of inhibiting chitin and 1,3-β-D-glucan synthesis in ras and calcineurin mutants of *Aspergillus fumigatus*. *Antimicrob. Agents Chemother.* **53,** 476–482
59. Valiante, V., Jain, R., Heinekamp, T., and Brakhage, A. A. (2009) The MpkA MAP kinase module regulates cell wall integrity signaling and pyomelanin formation in *Aspergillus fumigatus*. *Fungal Genet. Biol.* **46,** 909–918
60. Alam, M. K., and Kaminskyj, S. G. W. (2013) *Aspergillus* galactose metabolism is more complex than that of *Saccharomyces*: the story of GalD-GAL7 and GalEGAL1. *Botany* **91,** 467–477
61. Alam, M. K., El-Ganiny, A. M., Afroz, S., Sanders, D. A., Liu, J., and Kaminskyj, S. G. (2012) *Aspergillus nidulans* galactofuranose biosynthesis affects antifungal drug sensitivity. *Fungal Genet. Biol.* **49,** 1033–1043
62. Timson, D. J. (2007) Galactose metabolism in *Saccharomyces cerevisiae*. *Dyn. Biochem. Process Biotech. Mol. Biol.* **1,** 63–73
63. Slepak, T., Tang, M., Addo, F., and Lai, K. (2005) Intracellular galactose 1-phosphate accumulation leads to environmental stress response in yeast model. *Mol. Genet. Metab.* **86,** 360–371
64. Mellado, E., Dubreucq, G., Mol, P., Sarfati, J., Paris, S., Diaquin, M., Holden, D. W., Rodriguez-Tudela, J. L., and Latgé, J. P. (2003) Cell wall biogenesis in a double chitin synthase mutant (chsG−/chsE−) of *Aspergillus fumigatus*. *Fungal Genet. Biol.* **38,** 98–109
65. Gastebois, A., Mouyna, I., Simenel, C., Clavaud, C., Coddeville, B., Delepierre, M., Latgé, J.-P., and Fontaine, T. (2010) Characterization of a new β(1–3)-glucan branching activity of *Aspergillus fumigatus*. *J. Biol. Chem.* **285,** 2386–2396